J Biochem Tech (2018) 9(4): 9-14
ISSN: 0974-2328

An Effect of Calcination Temperatures on the Characteristics of the $Mgfe_2o_4$ Nano Ferrite Prepared Using Auto Combustion Method

Ahmed Yaseen*, Tahseen. H. Mubarak, Sabah M. Ali Ridha

Received: 18 June 2018 / Received in revised form: 27 October 2018, Accepted: 28 October 2018, Published online: 17 December 2018

Abstract

Nanosized magnesium ferrite $MgFe_2O_4$ was synthesized using sol-gel auto combustion method as a burnt powder calcined at different temperatures (350, 500, 650, 800 and 950 C˚). These powders were pressed into a disk shape compact, and sintered at 1100 C˚ for 3 hours. The X-ray diffraction patterns of the ferrite powders showed the formation of spinal cubic structure, whereas the crystallite size increased with increasing calcined temperatures from 29 to 42 nm. The absorption bands of the FTIR spectra of all the ferrite powders showed that the magnesium ferrite had two absorption bands within the range of (408.9 – 563.2 cm^{-1}) for high and low frequencies. The dielectric constant, dielectric loss and ac conductivity for the sample sintered at (1100 C˚) were studied as a function of frequency at room temperature by using LCR meter. The variation of dielectric properties at frequencies from 50Hz to 1MHz has been explained on the basis of Koop's theory. Maxwell-Wagner polarization process at hopping of electrons for all the dielectric properties indicated normal behavior with increasing the frequency. The particle size represented by AFM was found to be within the range of (67.49 nm), and the square root of the average roughness was directly of proportional particle size and granular boundary limitations.

Keywords: Mg-Ferrite, Dielectric Properties, Nano Powders, Sol-Gel Auto Combustion Method.

Introduction

Nanomaterials have unique properties for commercial applications (Mahmoud, et al. 2018). Nanoparticles offer distinct properties such as particle size, increased chemical reactivity, and increased surface area/mass ratio compared to their bulk counterparts (Haripriya & Ajitha, 2017). Spinal ferrite materials with chemical formula ($MgFe_2O_4$) play a significant role in manufacturing the microwave control parts such as isolators, circulators and phase shifters (I. K. Jassim et al., 2013). Among different ferrites, magnesium ferrite has a special care because of high-density in recording media, it has great applications, heterogeneous catalysis, adsorption, magnetic technologies, and sensors (Z. Lazarevi, 2011). There are a lot of methods for synthesizing nano sized spinal ferrites, such as co-precipitation, sol-gel, ceramic and hydrothermal etc. (P.K. Roy, 2006). The ferrite has an ability to reduce energy dissipation due to the reduction cycle of remanence and it has high electrical resistance that distinguishes it from the other metals, it is also used in communications equipment receiving and broadcasting circuits), filters in the radar , antenna bars , magnetic amplifiers , digital cameras, and computer memories (Rawnaq B. J., 2018; N.H.Alwash, 2009). In the present work, magnesium ferrite nano powders were prepared by sol-gel auto combustion method, and the structural and dielectric characteristics were studied by using XRD, FTIR, LCR meter, and AFM instruments.

Ahmed Yaseen*, Tahseen. H. Mubarak

Department of Physics, College of Sciences, University of Diyala, Iraq

Sabah M. Ali Ridha

Department of Physics, College of Education for Pure Sciences, University of Kirkuk, Iraq

***E-mail:** Ahmedyassin057 @ gmail.com

Experimental Method

Nano magnesium ferrite was prepared by using sol-gel method with chemical formula of $MgFe_2O_4$. The stoichiometric amount of ferric nitrate Fe $(NO_3)_3.9H_2O$, magnesium nitrate Mg $(NO_3)_2.6H_2O$ and citric acid $C_6H_8O_7$ were dissolved separately in (30-40mL) of deionized water to obtain a clear solution without any heating processes. Then, ammonia solution was added until getting (pH=7), after that, the temperature of the magnetic stirrer was gradually increased to (90 C˚) for (2h) with continuous stirring to obtain a viscous brown gel. The viscous gel was dried in an electric oven, and left until the combustion of dry gel was seen completely, and as-burnt ferrite nano powder was produced. The as-burnt powder was calcined at various temperatures of 350, 500, 650, 800, and 950 C˚ for 3 hours. For studying the dielectric characteristics, the as-burnt powders were pressed into circular pellets of diameter (12mm) with thickness about (2mm) by applying the pressure of (2.5 tons/cm^2) using hydraulic pressure. These pallets were sintered at (1100 C˚) for 3 hours to obtain the samples for dielectric properties.

Table 1: The weight ratios used to prepare the sol -gel state

Materials	$Fe(NO_3)_3 9H_2 0$	$Mg(No_3)_2 6H_2 o$	$C_6H_8O_7$
Weight of materials (gm)	40.4	12.82	28.8

Results and Discussion

Structural properties

Fig (1) shows the XR diffraction pattern of the prepared samples (c1, c2, c3, c4, c5, c6) that confirms the formation of spinel cubic structure. The x-ray diffraction pattern indicated that seven clear peaks were found considering the nature of the crystalline composition for mgfe2o4 which proved to be (fcc) and its correspondence to the standard pattern with reference to co de (ICDD-o17-o464).

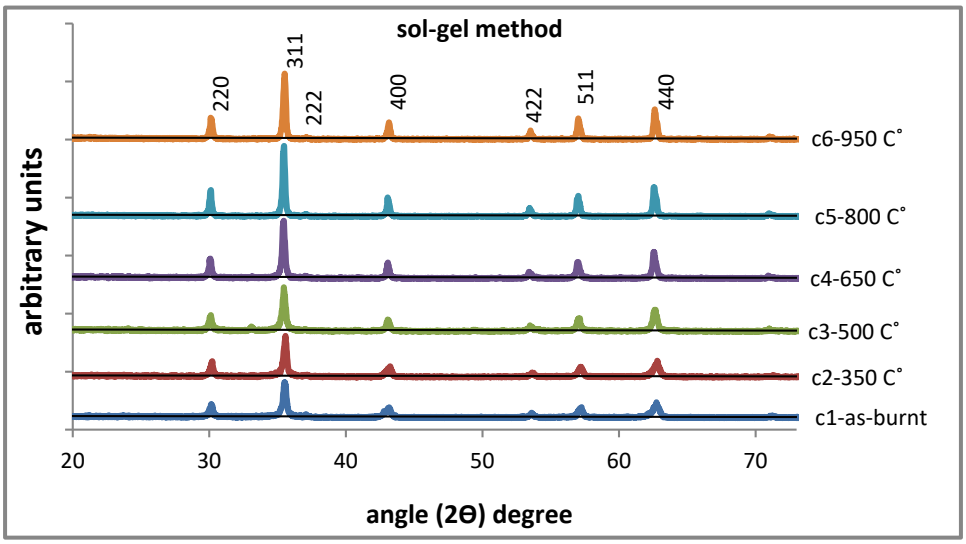

Fig. 1: X-ray diffraction patterns of magnesium ferrite powders

The lattice constant (a) of the Mg- ferrite was equal to 8.37A˚, and it was calculated by using Braggs equation (B.k.Nath, 2005).

$$a = d_{hkl}\sqrt{h^2 + k^2 + l^2} \qquad (1)$$

Where, (h, k, l) are the miller indices, (d) is spacing between the planes , (a) is the lattice constant in (A˚) units. In this study, magnesium ferrite had a single phase (S. M. Rathod, 2012), referring to the spinel structure with a standard card (ICDD-36-0398) (A. Pradeep, 2008).

Crystallite size, lattice constant, and X-ray density of all the samples were calculated for the intense peak (311), as a function of the calcined temperature as shown in figure (2) and listed in table (2). The crystallite size increased with increasing the calcination temperatures, due to the recrystallization of the Mg-ferrite samples, and lattice constant was decreased with increasing calcined temperatures. All these changes tended to be slightly increasing based on X-ray density.

$$D = \frac{k\lambda}{\beta_{hkl} cos\theta} \qquad (2)$$

Where D is the crystallite size, B is the full width half maximum of the peak (311), λ is the wavelength of Cu-kα, and θ is the Braggs angle.

Table 2: Lattice parameter, crystallite size, and X-ray density for the intense peak (311)

sample	lattaice constant (a)A°	Crystallite size (D) nm	Density *P* (g/cm^3)
C1	8.379198467	29.4486865	4.516185793
C2	8.374564867	30.1427725	4.523686282
C3	8.372284286	32.5156642	4.527383998
C4	8.369572095	38.3836607	4.531786772
C5	8.372466684	42.5352965	4.527088111
C6	8.369572095	44.1163307	4.531786772

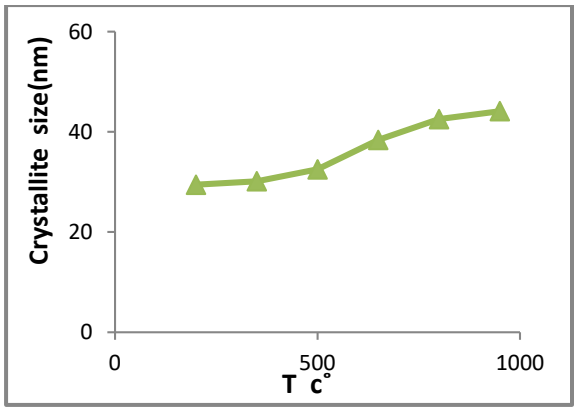

Fig. 2: The change of crystallite size with temperature

Data in table (3) shows the hopping length in A-site (L_A) tetrahedral and B-site (L_B) octahedral according to the relations below;

$$L_A = 0.25a\sqrt{3} \quad (3)$$

$$L_B = 0.25a\sqrt{2} \quad (4)$$

In Mg-ferrites, (Fe^{+2}) ion behaved as a semiconductor of n-type, while Fe^{+3} ion behaved as p-type.

Table 3: The electronic hoping length values of the two groups (L_A, L_B)

Ferrites calcined at different temp.	L_A (°A)	L_B (°A)
C1	3.628	2.9625
C2	3.626	2.9609
C3	3.625	2.96
C4	3.624	2.9591
C5	3.625	2.9601
C6	3.624	2.9591

FTIR spectra

Figure (3) shows the infrared spectra analysis of $MgFe_2O_4$. It is an important means that confirms the formation of the spinel structure, and the spectrum gives not only the location of the ions in the lattice, but also shows their vibration patterns.

The absorption bands of the FTIR spectra occur by the vibration of oxygen ions with the ketones found in the octahedral and tetrahedral sites in the spinel structures. In this study, magnesium ferrite had two absorption bands within the range of (408.9 – 563.2 cm^{-1}) for high and low frequencies respectively as shown in table (4), (L. S. Mahmood, 2012).

The higher frequency bands (v1) at tetrahedral A-site were due to the stretching vibration of the unit cell with oxygen, and the lower frequency bands (v2) at octahedral B-site were caused by the metal-oxygen vibration (L. S. Mahmood, 2012).

Table 4: shows the absorption frequencies of FTIR rays

Preparation Method	Temp. C°	U_1 cm^{-1}	U_2 cm^{-1}
Sol-gel (C-series)	as burn	412.766	561.285
	350	410.837	557.427
	500	408.908	563.214
	650	408.908	563.214
	800	410.837	561.285
	950	410.766	559.356

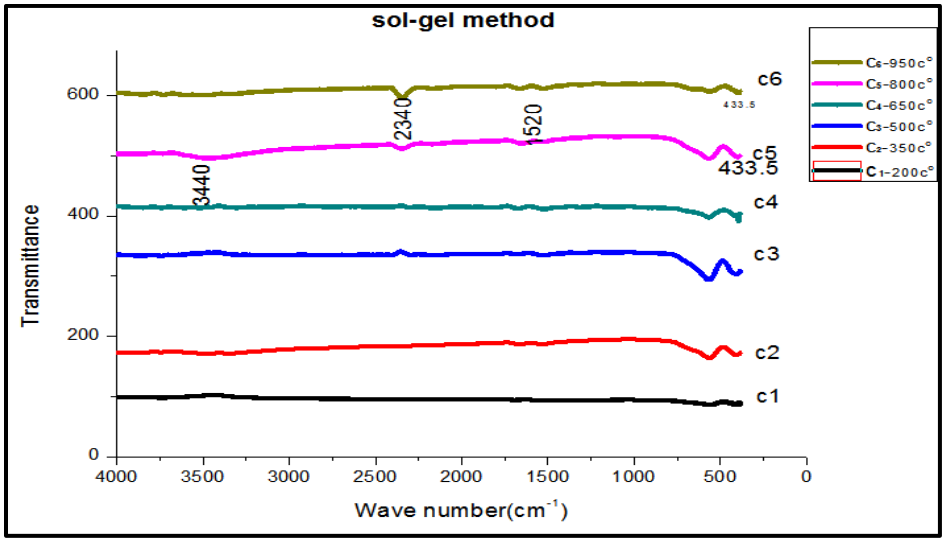

Fig. 3: The FTIR infrared spectrum

Atomic Force Microscopy (AFM)

The surface topography of the Mg-ferrite nano powders was studied using an atomic force microscope (AFM) with a high capacity for surface imaging and analysis at the range scale of (2

* 2μm²). The device gave statistical values on the particle size and the distribution as well as the surface roughness values, based on the square root of the Mean Square (RMS) which reached (9.13 nm) (S. Thankachan, 2013). In figure (4), the particle size was found to be within the nano-range of (67.49nm) and the square root of the average roughness.

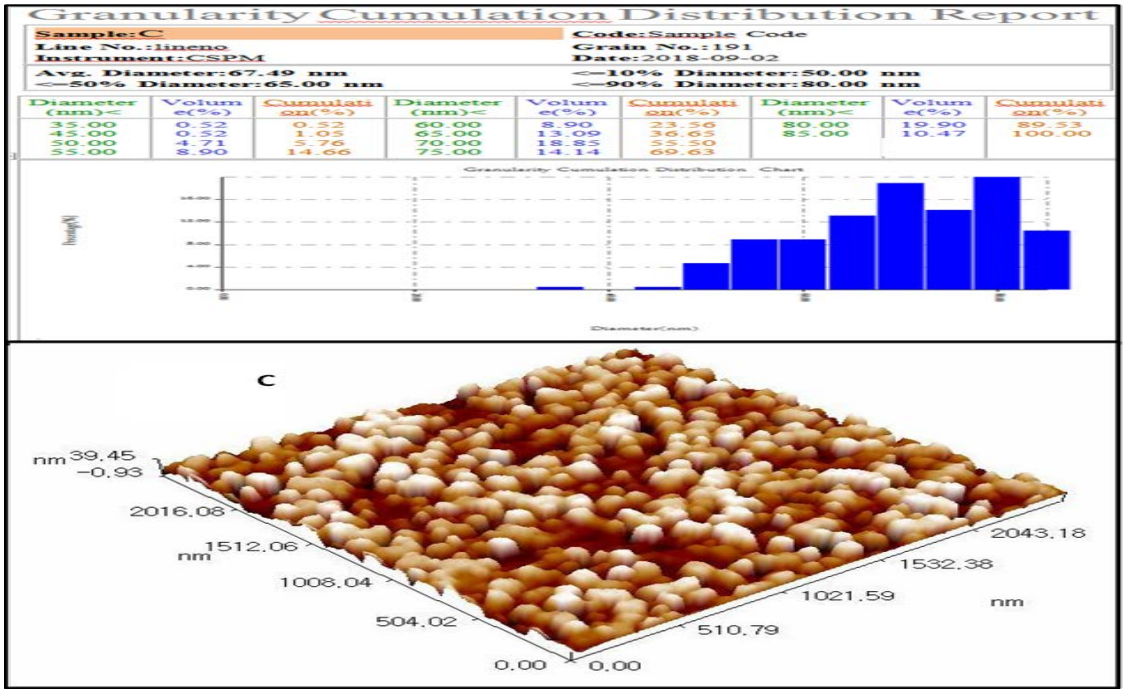

Fig. 4: AFM image with particle size chart and distribution by volume ratios

Electrical Properties

- *Dielectric constant $\mathcal{E}'$*

Figure (5) shows the change in the values of dielectric constant as a function of the frequency in the range of (50Hz to 1MHz) at room temperature, it concluded the increasing frequency with decreasing dielectric constant, and it was calculated by the equation (5).

$$\mathcal{E}' = \frac{C_p d}{\varepsilon_0 A} \qquad (5)$$

Where (ε') is the real part of dielectric constant, (d) is the thickness of the pellet in meter, (C_p) is the capacitance of the pellet in farad, (ε_0) is the constant of permittivity of free space, A is the cross – sectional area of the flat surface of the pellet.

This behavior was considered normal for all types of ferrite as observed by many researchers, (M.N. Ashiq, 2009) because of the movement of charges and dipoles, which is unable to change its direction with the electric field, and therefore lag behind it which leads to decrease the electric polarization, and then decrease the dielectric constant as listed in table (5), (L. S. Mahmood, 2012).

Table 5: The change in the values of the insulation constant for three frequencies

Preparation method for samples	Dielectric constant'(ε')at (200KHz)	Dielectric constant'(ε')at (200KHz)	Dielectric constant'(ε')at (200KHz)
sol-gel	4.767476	4.635302	4.551082

Figure (6) shows the change of ac conductivity ($\sigma_{a.c}$) as a function of frequency at room temperature calculated by equation (6).

$$\sigma_{A.C} = 2\pi f \varepsilon_0 \mathcal{E}' \tan\delta \qquad (6)$$

Where f is the frequency and tanδ is the dielectric loss angle.

The ac conductivity gradually increases with frequency, and slowly increases at higher frequencies, the reason is that the grain boundaries at lower frequencies are more effective than the grains for electric conduction, therefore, the hopping length of Fe2+ and Fe3+ ions are bound at lower frequencies (Gh. Khalaf. Salman, 2012).

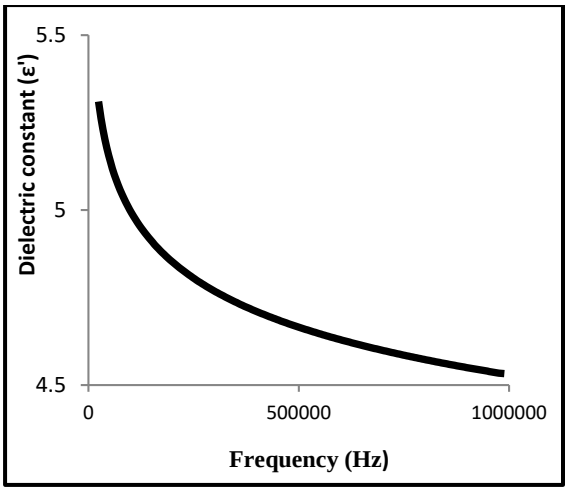

Fig. 5: The Dielectric constant with frequency

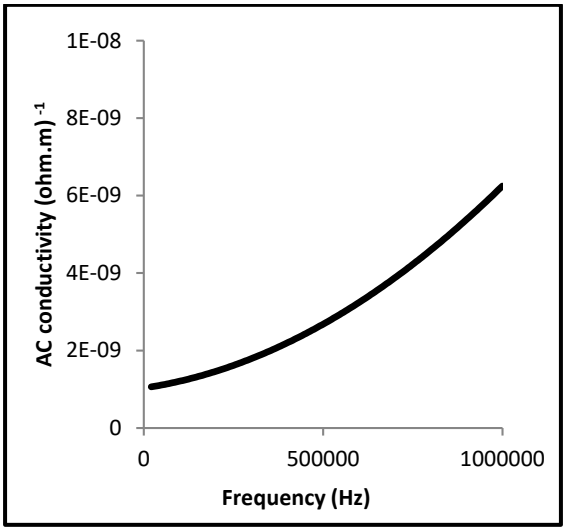

Fig. 6: A.C conductivity with frequency

- *Dielectric loss factor (Ɛ″)*

It is possible to calculate the coefficient of Dielectric loss factor (Ɛ″) by equation (7), which is directly proportional to the dissipation of energy in the insulation materials. This factor is of great importance in the applications of the ferrite material to determine the final operating frequency in the magnetic materials has been observed the highest value of the dielectric loss factor at low frequencies and decreases by increasing the frequency of electric field (Gh. Khalaf. Salman, 2012).

$$Ɛ'' = Ɛ' \tan\delta \qquad (7)$$

Where Ɛ´´, imaginary part of the dielectric constant.

Figure (7) shows the inverse proportional between the Dielectric loss factor (Ɛ″) and frequency. This is due to the large energy absorbed by the dipoles from the electric field, which increases the possibility of collisions between the electrodes during the rotation at low frequencies resulting in the possibility of weakening the electrical insulation. When the amplitude of the applied field is increased, the dipoles' ability to follow the change of the electric field decreases, thus reducing the energy absorbed by the dipoles from the electric field, which results in a decrease in the dielectric loss factor with increased frequency of the electric field (A. M., Mohammad, 2018).

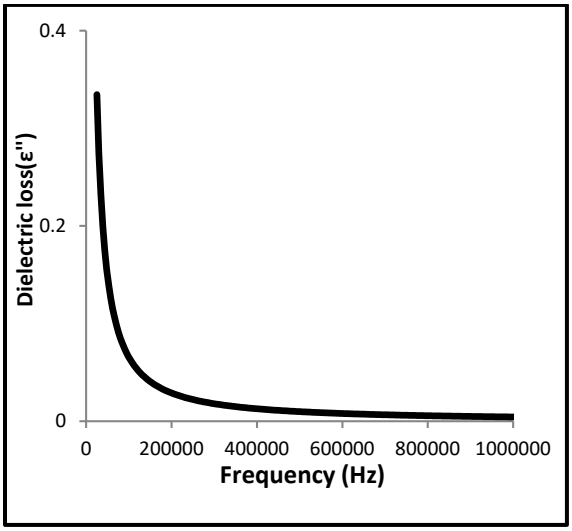

Fig. 7: The change in the Dielectric loss factor with the frequency range (50 Hz-1MHz)

Conclusion

In the present study, the variation of dielectric properties at frequencies from 50Hz to 1MHz has been explained on the basis of Koop's theory. Maxwell-Wagner polarization process at hopping of electrons for all the dielectric properties indicated normal behavior with increasing the frequency. The particle size identified by AFM was found to be within the range of (67.49 nm), and the square root of the average roughness was directly of proportional particle size and granular boundary limitations.

References

A. M., Mohammad, S. M. A. Ridha, , & T. H. Mubarak, (2018). Dielectric Properties of Cr-Substituted Cobalt Ferrite Nanoparticles Synthesis by Citrate-Gel Auto Combustion Method. International Journal of Applied Engineering Research, 13(8), 6026-6035.

A. Pradeep, P. Priyadharsini, & G. Chandrasekaran, (2008). Sol–gel route of synthesis of nanoparticles of MgFe2O4 and XRD, FTIR and VSM study. Journal of Magnetism and Magnetic Materials, 320(21), 2774-2779.

B.k.Nath,P.K.Chakrabarti,S.das,U.kumr,P.K.Mukhopadhyayand D.das., surface sci. techno. vol.21, No. 3-4, pp. 169-182 (2005).

Gh. Khalaf. Salman, "preparation and study the characteristics of magnesium ferrite materials" M.Sc. thesis, school of applied sciences, university of technology, 2012.

Haripriya S, Ajitha P. Antimicrobial efficacy of silver nanoparticles of Aloe vera. J Adv Pharm Edu Res 2017;7(2):163-167.

I. K. Jassim, R. A. mohammad & H. MK. Farage "The Effect of Heat Treatment on The Magnetic properties of The (Fe-Ni) Alloys Prepared by powder Metallurgy Method" Vol. 18, No. 2, pp.,244-248, (2013)

L. S. Mahmood," Preparation of Co1-xZnxFe2O4 nano ferrite and study of its electrical and structural properties" Scientific Research University of Diyala College of Science Department of Physics, P(63,64),(2012) .

Mahmoud,Z. Hassan, K.H. Abdul Sattar, O.D. & Kefah Ali,F. Low Temperature Novel Photosynthesis Method and Characterization of ZnO/CuO Nano composite. J Biochem Tech (2018) 9(3): 1-4.

M.N. Ashiq," Effect on Physical, Electrical and Magnetic Properties of Strontium Hex ferrite Nanomaterial Doped with Binary Mixtures of Various Metal Ions", Ph.D thesis, University Islamabad ,4-14,(2009).

N.H.Alwash," The effect of sintering time on the magnetic properties Ni 1-x ZnxFe2O4 for the syntheses", The Iraqi Journal For Mechanical And Material Engineering,(c), 499-511 , (2009).

P.K. Roy," Enhancement of the magnetic properties of Ni–Cu–Zn ferrites with the substitution of a small fraction of lanthanum for iron", National Institute of Technology Journal, 42(1), 77-83,(2006).

Rawnaq B. J., Zaid H. M., Farah K. A., Evaluation the efficiency of CuFe2O4 prepared photolysis by OSD and photo degradation, Entomol Appl Sci Lett, 2018, 5 (2): 91-100.

S. M. Rathod," Synthesis and characterization of Nano crystalline NiCuZn Ferrite prepared by Sol-gel auto combustion method". International Journal of Advancements in Research and Technology, 6(1), 2278-7763, (2012).

S. Thankachan, S. Xavier, B. Jacob, & E. M. Mohammed, (2013). A comparative study of structural, electrical and magnetic properties of magnesium ferrite nanoparticles synthesized by sol-gel and co-precipitation techniques. Journal of experimental Nanoscience, 8(3), 347-357.

Z. Lazarevi," Preparation and Characterization of Nano Ferrites", Acto Physical polonica Journal, 3(121), 682-687, (2011).